

Original articles

Research article

<https://doi.org/10.17308/kcmf.2024.26/11809>

Isolation of partial coupled processes of anodic oxidation of OH⁻ ion on gold using a combination of a graph-kinetic analysis method and linear voltammetry data

I. D. Zartsyn, A. V. Vvedenskii, E. V. Bobrinskaya , O. A. Kozaderov

Voronezh State University,
1 Universitetskaya pl., Voronezh 394018, Russian Federation

Abstract

The presence of several interconnected electrochemical processes occurring on the surface of an electrode, strictly speaking, does not allow the use of the principle of independent reactions. Often, partial reactions of a complex multi-stage electrochemical process are coupled both through common intermediates and through the competitive adsorption of electroactive species. The presence of conjugation leads either to a change in the potential at which the corresponding electrochemical process becomes possible or to a change in the rate of partial processes. The latter is called kinetic coupling. This does not allow the simple calculation of the rate of each partial reaction as the difference between the current density of the target and background processes. The method of kinetic diagrams can be used to establish the kinetic patterns of such processes. This study shows that this method is applicable not only for the analysis of coupled electrochemical processes of various types, but can also be used in obtaining partial currents of the stages of a separate complex electrode reaction occurring in a background solution. As an example, options for the kinetic modelling of the total voltammogram of the anodic process on an Au electrode in an aqueous alkaline medium in the mode of linear potential change are considered.

The stationary degrees of covering of the gold surface with various surface-active forms of oxygen are calculated depending on the electrode potential. It was established that the change in concentration of OH⁻ ions mainly affects the region of their adsorption potentials. A detailed analysis of stationary partial anodic processes in the Au|OH⁻, H₂O system was carried out and the shape of the general stationary voltammogram was determined by calculation. The latter is in qualitative agreement with the experimental polarization dependence.

It was shown that the type of calculated polarization dependence is determined by the degree of reversibility of individual stages and the rate of their occurrence. The performed analysis is necessary not only for the detailed scheme of the background anodic reaction on gold in an alkaline solution, but also for the subsequent kinetic description of the electrooxidation process of organic substances on a gold electrode.

Keywords: Electrode processes, Conjugation, Graphic-kinetic analysis, Adsorption, Voltammetry

Funding: The study received financial support from the Ministry of Science and Higher Education of the Russian Federation within the framework of State Contract with universities regarding scientific research in 2022–2024, project No. FZGU-2022-0003.

For citation: Zartsyn I. D., Vvedenskii A. V., Bobrinskaya E. V., Kozaderov O. A. Isolation of partial coupled processes of anodic oxidation of OH⁻ ion on gold using a combination of a graph-kinetic analysis method and linear voltammetry data. *Condensed Matter and Interphases*. 2024;26(1): 55–67. <https://doi.org/10.17308/kcmf.2024.26/11809>

Для цитирования: Зарцын И. Д., Введенский А. В., Бобринская Е. В., Козадеров О. А. Выделение парциальных сопряженных процессов анодного окисления OH⁻-аниона на золоте сочетанием метода графо-кинетического анализа и данных линейной вольтамперометрии. *Конденсированные среды и межфазные границы*. 2024;26(1): 55–67. <https://doi.org/10.17308/kcmf.2024.26/11809>

 Elena V. Bobrinskaya, e-mail: elena173.68@mail.ru

© Zartsyn I. D., Vvedenskii A. V., Bobrinskaya E. V., Kozaderov O. A., 2024



The content is available under Creative Commons Attribution 4.0 License.

1. Introduction

When several multi-stage reactions simultaneously occur on the electrode surface, in the same potential region and at comparable rates, then the partial reactions are not independent. Usually they are interconnected (coupled) not only via common intermediates, but also due to the competition of different electroactive particles for adsorption centres.

The presence of conjugation provides the possibility of transferring the free energy of the electrode system between partial reactions, due to which some of them acquire the ability to take place at potentials more negative than the corresponding equilibrium potentials - thermodynamic coupling [1]. More often, however, only the rate of each of the partial processes changes accordingly, there is kinetic coupling [2,3].

The problem of coupled reactions is primarily associated with the problem of finding real partial rates, and therefore with establishing kinetics. Indeed, in the simplest case, only two interconnected processes occur on the electrode, target (1) and background (2), both in a non-diffusion mode. If i_1 and i_2 are the partial rates of each process, i.e., rates obtained taking into account coupling effects, then $i = i_1 + i_2$. Here i is the current measured in the external polarization circuit; the nature of its change over time is not important for subsequent consideration.

Often $i_2^{\text{background}}$ is used as i_2 , this is the current determined in the same potential region, but in the background electrolyte instead of the working one, containing an electrochemically active reagent. However, due to coupling $i_2 \neq i_2^{\text{background}}$, and therefore the i values often are determined with a noticeable error.

A typical example is the processes of anodic oxidation of organic substances on metal electrodes, which are also capable of anodic oxidation during polarization. Often, the areas of adsorption potential and electrochemical activity of organic substances and the metal substrate overlap, which predetermines the potential for the mutual influence of partial electrode processes [4–7]. In this situation, the graph-kinetic analysis method [8–11], where a multi-stage chemical process is represented as a set of interconnected cycles (graphs), is very useful. Due to the absence

of any significant internal limitations, the method is also applicable to electrochemical reactions occurring simultaneously on the electrode.

Such an analysis plays a special role in the study of complex electrochemical processes on metals and alloys in the presence of surfactants of various nature. Knowledge of the conjugation features of partial electrode processes in such systems makes it possible not only to theoretically describe the processes involving electrolyte solution components, but also to reasonably formulate technological principles for the production of electrochemical transformation products (including anodic oxidation of organic additives and cathodic deposition of metals and alloys) with specified properties and composition.

It is possible to obtain true partial currents by calculation by sequentially considering alternative kinetic situations that differ in the nature of the intermediates, the assumption about the nature of the limiting stage, or taking into account the presence of several stages with comparable rates and the sum of partial currents will provide the total i, E -dependence. This dependence is compared with an experimental voltammogram (VAG), allowing not only to estimate the complex of equilibrium and kinetic characteristics of individual stages, but also to draw a conclusion about the putative reaction scheme. It should be remembered that the graphic-kinetic analysis can also be used when interpreting the results of studies of individual electrode reactions.

Such reactions, usually, are complex and include the stages of adsorption, charge transfer, heterogeneous chemical transformations of intermediates, etc. In accordance with the assumed kinetic scheme of the general electrode process, its elementary stages successively replace each other as the potential changes.

On the other hand, an individual multi-stage electrode reaction can be interpreted only formally, as a set of “parallel” ongoing elementary processes, each of which corresponds to a separate stage, but is implemented over the entire range of potentials. The fact that in a certain range of potential values (E) the rates of elementary processes, conventionally considered as partial, are practically equal to zero, is not important

for this approach. It is much more important that it becomes possible to identify the partial currents of individual stages, summarize them, and compare the result with experiment, which usually underlies the refinement of the general reaction scheme and the identification of the kinetic features of a complex reaction.

Finally, it should be noted, that graph-kinetic analysis initially assumes a stationary course of a complex reaction, which is usually characteristic of homogeneous chemical processes. However, heterogeneous electrode reactions, in particular reactions studied by linear voltammetry, when the potential changes at a rate of $v = \frac{dE}{dt}$, are usually non-stationary.

The subject of this study is the electrode process occurring over a wide range of anodic potentials on a polycrystalline Au electrode in a deaerated aqueous alkaline solution. The main objectives of the study were:

- by calculation, using the method of graphic-kinetic modelling, determine the stationary covering degrees of the gold surface with the starting substance, intermediates and products of the anodic oxidation reaction of OH ions in an alkaline medium;
- calculate stationary partials, as well as the total anode current of this process;
- compare calculated and experimental values of a number of basic kinetic parameters of the anodic overall reaction in the Au|OH⁻,H₂O system;
- evaluate the correctness of the procedure for comparing the full calculated with the

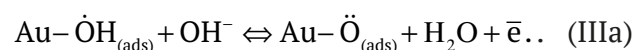
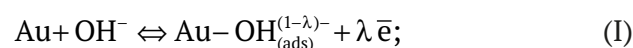
experimental voltammogram taken at a finite rate of potential change $v = \frac{dE}{dt}$.

2. Calculation procedure

2.1. Selection of reaction scheme

According to data [7], on the anodic branch of the cyclic i, E -dependence obtained in the Au|OH⁻,H₂O system four main current maxima can be distinguished – A1, A2, A3, and A4 (Fig. 1.). Since the regularities of cathodic processes are not considered in this study, the region of cathodic currents is not presented; potentials are given relative to SHE.

At higher v the amplitude of all current peaks increases, the potentials of the A1 and A2 maxima do not change, and the A3-A4 maxima shift to the region of more positive values. This finding, like other data [12–20], indicates a multi-stage anodic process in the Au|OH⁻,H₂O system. The latter proceeds via the chemisorption stage of the hydroxide anion, most likely with partial charge transfer, and is accompanied by the sequential formation of mono- and biradical forms of adsorbed atomic oxygen. A possible reaction scheme in the simplified form is:



Here λ - degree of partial charge transfer from an adsorbed particle with a charge $z = 1$ per metal; eventually $z_{\text{ads}} = 1 - \lambda$ [21]. It is assumed

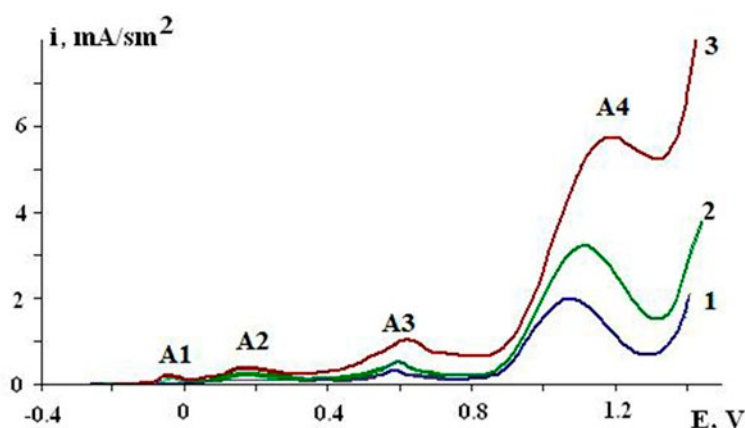
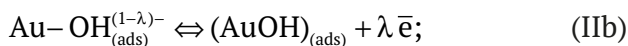


Fig. 1. Anode voltammograms experimentally obtained on a smooth gold electrode in 0.1 M NaOH solution at $v = 0.04$ (1); 0.1 (2) и 0.6 (3) V/sec [7]

[22–24] that the radical ion state is stabilized due to the overlap of 6s- and sp³- AO for Au and OH⁻, respectively. As an alternative, the appearance of 2D Au(I) and Au(II) compounds on the surface is possible in such processes as:



The formation of phase Au(III) oxide at sufficiently high potentials is the result of a series of sequential electrochemical, chemical, and crystallization stages. In overall form, the corresponding reaction can be represented as a process involving Au- $\ddot{\text{O}}_{(\text{ads})}$ or (AuO)_{ads}:



The formation of metastable phases, Au(OH) or γ -AuOOH, with subsequent dehydration, cannot be excluded; these issues are considered in more detail in [30].

The choice between alternative routes for anodic formation of Au₂O₃ via (IIa), (IIIa), and (IVa), or (IIb), (IIIb), and (IVb) stages, must be based on information about the physical nature of the intermediates, which is usually missing. Thus, the question about the nature of the electron density redistribution in the Au|OH⁻, H₂O system remains open: its “flow” from the oxygen of the hydroxide ion to the metal, stages (IIa) and (IIIa), or back from the metal to oxygen, stages (IIb) and (IIIb). The results of quantum chemical modelling [23], however, are in favour of the first scenario. Therefore, this scenario was used later on, during the stage of constructing graphs for the intermediates of heterogeneous processes of OH⁻ oxidation in the aquatic environment $\dot{\text{O}}\text{H}$ and $\ddot{\text{O}}$.

The potential range of anodic release of molecular oxygen, which further complicates oxide formation on gold in an alkaline medium, was not considered in the study.

2.2. Initial kinetic ratios

Let us assume that the surface of gold initially contains only one type of active adsorption centres. The number of these centres is G, expressed in mol/cm², it is not only constant, but also significantly less than the number of metal atoms. The latter allows ignoring, albeit to a first

approximation, the effects of lateral interactions between adsorbate particles, and therefore to use the Langmuir isotherm model in the analysis.

Let G_i and G_j be the number of active surface centres, expressed in mol/cm² occupied by particles of i-th and j-th types, and G is the total surface concentration of such centres, respectively. The change in the state of the active site during $i \rightarrow j$ process may be associated not only with the oxidation/reduction of particles, but also with their adsorption/desorption. Each of these processes is interpreted as a kinetically reversible first-order reaction, the rate of which is:

$$v_{ij} = k_{ij}\Gamma_i - k_{ji}\Gamma_j = \Gamma(k_{ij}\Theta_i - k_{ji}\Theta_j). \quad (1)$$

Here k_{ij} and k_{ji} are the formal rate constants, s⁻¹, A Θ_i and Θ_j are the proportion of surface adsorption centres occupied by reagents and products, respectively. We believe that there are no diffusion limitations for all types of particles; features of the structure of the electrical double layer and their influence on k_{ij} and k_{ji}, are not explicitly taken into account.

The current covering of adsorption centres is assumed to be stationary. In this approximation

$$\sum_i k_{ij}\Theta_i = \sum_j k_{ji}\Theta_j, \quad (2)$$

actually representing the so-called stationary kinetic adsorption isotherm, and

$$\sum_i \Theta_i + \sum_j \Theta_j = 1. \quad (3)$$

Since in this case k_{ij} = k_{ij}⁰c_i^v, k_{ji} = k_{ji}⁰c_j^v, then the concentration constant of adsorption equilibrium K_{ij} = k_{ij} / k_{ji} = K_{ij}⁰(c_i^v / c_j^v). K_{ij}⁰ = k_{ij}⁰ / k_{ji}⁰ is the standard equilibrium constant, and c^v is the volumetric molar concentration, expressed in mol/cm³.

Taking into account the possibility of partial charge transfer, the rate constants of adsorption stages involving singly charged anions are:

$$k_{ij} = k_{ij}^0(E^0)c_i^v \exp[\lambda\beta F(E - E^0)/RT]; \quad (4a)$$

$$k_{ji} = k_{ji}^0(E^0)c_j^v \exp[-\lambda\alpha F(E - E^0)/RT], \quad (4b)$$

whereas for electrochemical stages:

$$k_{ij} = k_{ij}^0(E^0)c_i^v \exp[(1 - \lambda)\beta F(E - E^0)/RT]; \quad (5a)$$

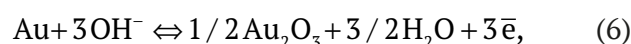
$$k_{ji} = k_{ji}^0(E^0)c_j^v \exp[-(1 - \lambda)\alpha F(E - E^0)/RT]. \quad (5b)$$

Here E and E^0 are the current and standard electrode potentials for a given reaction; a and b cathode and anodic charge transfer coefficients, respectively; everywhere further $a = b = 0.5$. If the adsorption of a charged particle is not accompanied by a redistribution of electron density, and therefore $\lambda = 0$, then the influence of E on the rate constants of adsorption processes in equations (4a) and (4b) disappears, and formulas (5a) and (5b) take their usual form. It is obvious that in the general case the values of K_{ij} , K_{ji} also depend on the potential, although to varying degrees.

3. Analysis of kinetic diagrams

3.3. Stationary reaction mode

According to the analysis technique proposed in [8–11] and detailed for electrode reactions in [2, 3], a kinetic diagram of the anodic process on the Au electrode in a background alkaline electrolyte was constructed (Fig. 2). The active centre of the gold surface, initially occupied by a water molecule was taken as the initial state (1); the vertices of the graph (2), (3), (4), and (5) correspond to the sequential formation $\text{Au}-\text{OH}_{\text{ads}}^-$, $\text{Au}-\dot{\text{O}}_{\text{ads}}$, $\text{Au}-\ddot{\text{O}}_{\text{ads}}$. Each of these processes, previously presented as (I), (IIa), (IIIa), and (IVa), has a corresponding graph edge. The covering of the surface with a certain adsorbate is, respectively, Θ_1 , Θ_2 , Θ_3 , Θ_4 , and Θ_5 ; traversing the loop counterclockwise is considered positive. Kinetically reversible overall reaction:



representing the sum of stages (I), (IIa), (IIIa), and (IVa), proceeds at the rate:

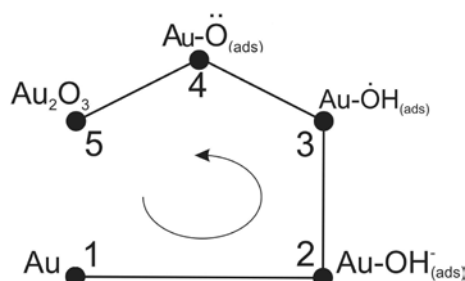


Fig. 2. Kinetic diagram of adsorption and electrochemical processes occurring on an Au electrode in an alkaline medium in the region of potentials preceding the anodic release of molecular oxygen

$$i_{15} = 3F(k_{15}\Theta_1 - k_{51}\Theta_5). \quad (7)$$

A detailed mathematical justification for the method of graph-kinetic analysis is described in detail in [34] and is not given within the framework of this study.

During the first stage, stationary degrees of surface covering with adsorbate particles were determined:

$$\Theta_1 = \frac{1}{1 + K_{12} + K_{12}K_{23} + K_{12}K_{23}K_{34} + K_{12}K_{23}K_{34}K_{45}}; \quad (8)$$

$$\Theta_2 = \frac{1}{1 + K_{21} + K_{23} + K_{23}K_{34} + K_{23}K_{34}K_{45}}; \quad (9)$$

$$\Theta_3 = \frac{1}{1 + K_{21}K_{32} + K_{32} + K_{34} + K_{34}K_{45}}; \quad (10)$$

$$\Theta_4 = \frac{1}{1 + K_{21}K_{32}K_{43} + K_{32}K_{43} + K_{43} + K_{45}}; \quad (11)$$

$$\Theta_5 = \frac{1}{1 + K_{21}K_{32}K_{43}K_{54} + K_{32}K_{43}K_{54} + K_{43}K_{54}}. \quad (12)$$

It is important that the meaning of the denominator in equations (8)–(12) is the same: each of them contains the concentration equilibrium constants of the transition processes from a given i -th state into all other states. The equilibrium constant values required for the calculation were determined by a brute-force search method.

It was found that the surface coverage of each of the adsorbed forms of oxygen, as expected, significantly depends on the electrode potential (Fig. 3a). It is very important that different potential regions can correspond to the presence of either one or the coexistence of several adsorbed forms. Thus, up to the values of $E \leq 0.3$ V the surface is covered only with adsorbed OH⁻ ions. With a further increase in the potential the surface coverage with the second adsorbed form also becomes non-zero, namely, $\dot{\text{O}}_{\text{ads}}$, and at $E \approx 0.7$ V, the degree of covering with this particle reaches unity. The subsequent increase in E leads to the appearance of biradicals $\ddot{\text{O}}_{\text{ads}}$ on the gold surface, the covering with which is very small and, moreover, noticeably decreases with increasing electrode

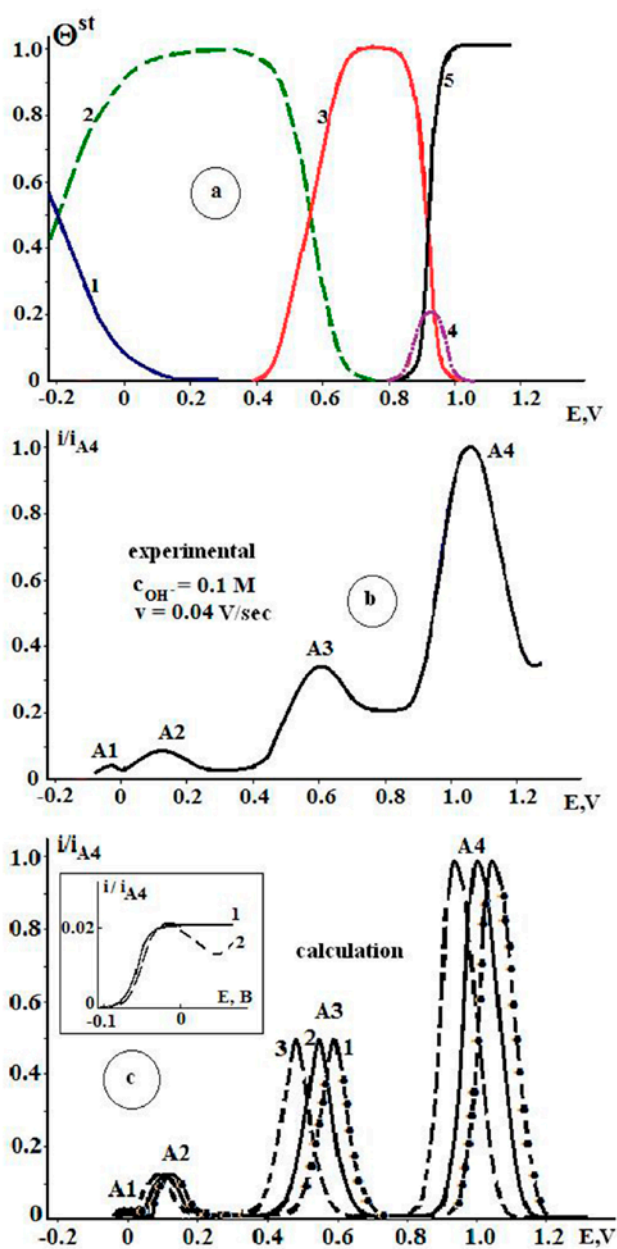


Fig. 3. a) The dependence of the stationary degrees of covering of the gold surface with various adsorbed forms and oxygen compounds at SN = 0.1 M: (1) – the initial surface, (2) – OH⁻, (3) – OH[•], (4) – O[•], (5) – Au₂O₃; b) Experimental voltammogram, obtained in the Au|OH⁻, H₂O [7] system and normalized to the maximum current A4; c) Calculated voltammograms normalized to the maximum current A4, with an alkali concentration equal to (1) – 0.1; (2) – 0.5 and (3) – 0.7 M. Inset: Area of the potential of maximum A1 without taking into account partial charge transfer during adsorption of hydroxide ion (1), as well as taking into account this process (2)

potential and the accumulation of Au₂O₃ occurs. An increase in the concentration of an alkaline solution from 0.1 M to 1.0 M manifests only as a slight expansion of the range of adsorption potentials of hydroxyl ions (not reflected in Fig. 3a), but practically does not affect the degree of surface covering with other adsorbed forms of oxygen.

The comparison of the potential regions of the maxima observed on the anodic branch of the experimental voltammogram, normalized to the current in the A4 maximum (Fig. 3b) with the corresponding regions of existence of various adsorbed forms of oxygen indicates that:

- A1 and A2 maxima characterize the process of adsorption of H₂O and OH⁻ ions respectively;
- in the region of A3 maximum, adsorbed OH⁻ ions and monoradicals OH[•] are present on the Au surface, and the anodic maximum corresponds to an almost equal covering of the electrode with each particle;
- potential region A4 corresponds to the coexistence of three adsorbed particles at once, and the maximum corresponds to the almost complete covering of the surface with gold oxide.

At the second stage of the analysis of the stationary anodic process in the Au|OH⁻, H₂O system, the rate v_i of each partial reaction and, accordingly, the corresponding partial current, were determined using the expression:

$$i_i = z_i F \Gamma v_i = z_i F \Gamma v \frac{d\Theta^{st}}{dE}, \tag{13}$$

Here it is taken into account that $dE = v dt$, and for a heterogeneous reaction of the first order $v_i = d\Theta_i/dt$. we assumed that as the potential changes, the covering of the surface with each particle of i -th grade stabilizes very quickly, i.e., the rate of potential scanning is significantly less than the speed of achieving stationary covering with adsorbate.

Expressions for partial currents were obtained by differentiating relations (8)–(12) with respect to potential, and then expressions for partial currents were found, using (4a)÷(5b). Their summation provides the desired i, E -dependence, which is quite cumbersome. For example, just one expression for $d\Theta_2^{st} / dE$, is this:

$$\frac{d\Theta_2^{st}}{dE} = \frac{F}{RT} \left[\frac{K_{21}^0 c_{OH^-}^{-1} \lambda \exp\left(-\frac{\lambda FE}{RT}\right) - K_{23}^0 \exp\left(\frac{FE}{RT}\right) - 2K_{23}^0 K_{34}^0 c_{OH^-} \exp\left(\frac{2FE}{RT}\right) - 3K_{23}^0 K_{34}^0 K_{45}^0 c_{OH^-}^2 \exp\left(\frac{3FE}{RT}\right)}{\left(1 + K_{21}^0 c_{OH^-}^{-1} \exp\left(-\frac{\lambda FE}{RT}\right) + K_{23}^0 \exp\left(\frac{FE}{RT}\right) + K_{23}^0 K_{34}^0 c_{OH^-} \exp\left(\frac{2FE}{RT}\right) + K_{23}^0 K_{34}^0 K_{45}^0 c_{OH^-}^2 \exp\left(\frac{3FE}{RT}\right)\right)^2} \right] \quad (14)$$

Nevertheless, it has been established that the full calculated VAG also contains four characteristic current maxima. Unfortunately, direct comparison of calculated and experimental i, E -dependencies is impossible, since the G_i value used in the calculations a priori unknown. Therefore, the calculated VAG were subjected to comparative analysis, which, like the experimental ones, were normalized to the current at the A4 maximum; the corresponding data are presented in Fig. 3c.

It is important that the maximum A1 in the calculated voltammogram can still be obtained, but only under the assumption of partial charge transfer in process (I), i.e., assuming $\lambda \neq 0$. Otherwise, in this region of potentials at $(i/i_4), E$ the dependence a horizontal plateau appears (inset to Fig. 3c), which contradicts the experimental data.

At the same time, the number and position of current maxima in the calculated and experimental voltammograms coincide. Moreover, the nature of the influence of the concentration of the alkaline solution on the position of the anodic current maxima turned out to be similar for the calculated and experimentally obtained i, E -dependencies (Table 1).

Thus, the position of A1 and A2 peaks do not change with increasing c_{OH^-} (Fig. 3c, Table 1), the potentials of A3 and A4 peaks somewhat reduce, and the value of the parameter $dE_a^m/d \lg c_{OH^-}$, obtained from the calculated VAG, practically coincide with

the experimental value. Some differences in the shape of the experimental and calculated VAG during the transition from A3 to A4 peak are due to the fact that the calculated voltammogram was obtained under the assumption of an equilibrium distribution of adsorbed particles, which is hardly true under real conditions.

Based on the condition of matching the position of each of the calculated and experimental anodic maxima, the values of the standard equilibrium constants of individual stages were determined and presented in Table 2.

During the third stage of comparing the calculated and experimental data, the concentration of surface adsorption centres was already specified. Moreover, the Γ value was chosen in such a way that the amplitudes of the experimental and calculated VAG at the corresponding potential scanning rate coincided.

It has been established that the nature of the change in the amplitude of the anodic maxima on the experimental and calculated VAG with increasing v , up to $v = 1.0$ V/s, is almost the same. Thus, the amplitudes of all anodic maxima change linearly with increasing potential scanning speed (Fig. 4), and the slopes of the corresponding experimental $\lg i, \lg v$, the dependences not only practically coincide for the A1-A3 maxima, but are also close to unity (Table 3).

However, for the A4 maximum the pattern is more complicated: the experimental value of

Table 1. Values of the slopes of the dependence of the potential of the maxima on the concentration of OH⁻ ions: experimental (numerator) and calculated (denominator) value ($v = 0.04$ V/sec)

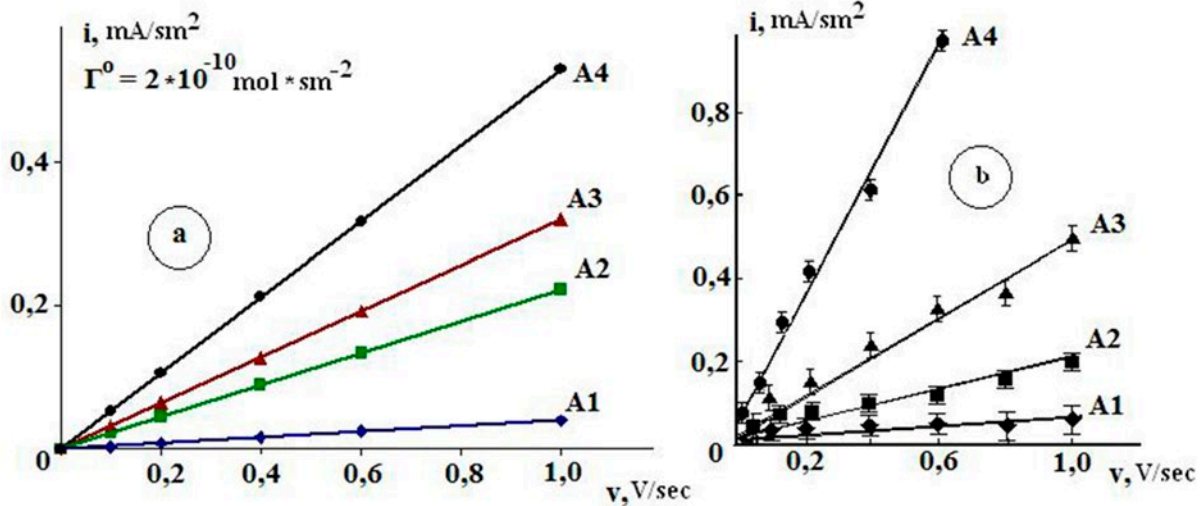
Parameter	A1	A2	A3	A4
Maximum				
$\frac{dE_a^m}{d \lg c_{OH^-}}, B$	$\frac{0}{0}$	$\frac{0}{0}$	$\frac{-0.043 \pm 0.004}{-0.045}$	$\frac{-0.062 \pm 0.005}{-0.075}$

Table 2. Concentration equilibrium constants of partial reactions occurring in the Au|OH⁻, H₂O system and presented in Fig. 2

Constant	Edge of the graph			
	(1↔2)	(2↔3)	(3↔4)	(4↔5)
K_{ij}^0	$1.5 \cdot 10^4$	$8.0 \cdot 10^{-11}$	$2.5 \cdot 10^{-13}$	$7.0 \cdot 10^{-13}$

Table 3. Values of the slope of the current in the maximum – scanning speed dependence of the in 0.1 M NaOH solution: experimental (numerator) and calculated (denominator)

Maximum Parameter	A1	A2	A3	A4
$\frac{d \lg i_a^m}{d \lg v}$	$\frac{0,87 \pm 0,08}{1.00}$	$\frac{0,83 \pm 0,08}{1.00}$	$\frac{0,85 \pm 0,08}{1.00}$	$\frac{0,62 \pm 0,06}{1.00}$


Fig. 4. Dependences of the current in the maximum of the voltammogram on the scanning speed of the potential: calculated (a) and experimental (b) [7] data

the parameter $\frac{d \lg i_a^m}{d \lg v}$ rather closer to 0.5, while

the calculated value, as for the others, is equal to unity. In our opinion, this discrepancy is due to the fact that the calculation takes into account the presence of only adsorbed Au₂O₃ oxide, whereas under the experimental conditions in the region of A4 maximum, a phase layer of Au(III) oxide is also most likely present on the surface [7; 12; 15; 31–32].

3.2. Unsteady reaction mode

Previously, it was experimentally established [7] that the potentials of the first two maxima, namely A1 and A2, are practically invariant to changes in the potential scanning rate up to $v > 8$ V/s, while the potentials of A3 and A4 peaks significantly improve with increasing v [7]. Naturally, the assumption used above about the stationarity of processes, primarily adsorption, occurring in the Au|OH⁻, H₂O system excludes the possibility of considering the influence of v to the position of current maximums. Therefore, a complete equation for a nonstationary anodic voltammogram, including the potential regions of all current maxima should be obtained.

However, solving this general problem is extremely difficult. Therefore, at first we will assume that heterogeneous adsorption processes occurring at the potentials of A1 and A2 peaks are quasi-stationary, while only processes in the region of potentials of A3 and A4 peaks are non-stationary.

A detailed procedure for taking into account nonstationarity effects using the graph method is presented in [33]. The kinetic diagram of a non-stationary process, taking into account the assumptions made, has a form similar to the stationary diagram (Fig. 2), but with additional branches (Fig. 5). Here 1 is a complex

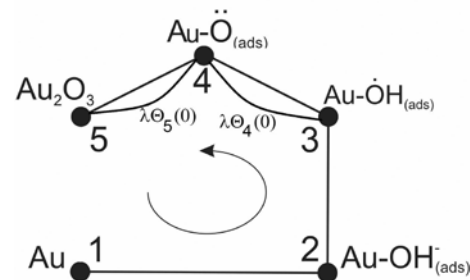

Fig. 5. Kinetic diagram of adsorption and electrochemical processes occurring on an Au electrode in an alkaline medium, taking into account the unsteadiness of processes in the potential range A3–A4

image of time. In this case, the rate constant of any non-stationary stage k_{ij}^* would be: $k_{ij}^* = k_{ij} + \lambda\Theta_j(0)$, and for the solution the Laplace–Carson transformation should be used [4, 34–35] under the assumption of a non-zero initial concentration of intermediate particles.

For further facilitation of the procedure of graphic-kinetic analysis, we will limit ourselves to considering only part of the general diagram presented in Fig. 2, assuming that adsorbed OH⁻ ions are initially present on the Au surface. Obviously, that in this case the region of their adsorption potentials falls out of consideration. Nevertheless, even within the framework of this simplification the situation remains very complicated, since the overall transformation process Au–OH_{ads}⁻ in Au₂O_{3(ads)} is a multi-stage process. Which of these elementary stages, or their combination, is slow and therefore determining the rate is not known a priori. Possible options are presented in Table 1. In addition to the anodic transformations of OH⁻ on gold with one limiting stage, situations with several rate-determining reactions are also considered here.

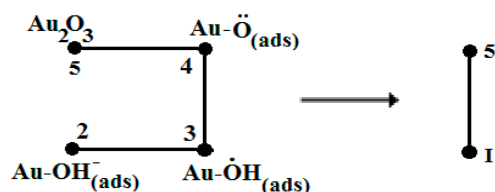
As an example, in this study we will limit ourselves to considering two kinetic scenarios from Table 4 – (a) and (b); both with a single rate-limiting stage.

Table 4. Alternative kinetic scenarios corresponding to the gross process of anodic transformation in the Au/OH⁻, H₂O system

Process scenario	Transformation scheme
(a)	(2) → (3) = (4) = (5)
(b)	(2) = (3) → (4) = (5)
(c)	(2) = (3) = (4) → (5)
(d)	(2) → (3) = (4) → (5)
(e)	(2) = (3) → (4) → (5)
(f)	(2) → (3) → (4) = (5)
(g)	(2) → (3) → (4) → (5)

Kinetic scenario (a)

We will use the graph technique and combine the elementary states (2), (3), and (4) into a formally initial state (I), which does not have a clear physical interpretation:



Now, to obtain the final equation of the voltammogram, it is enough to solve the differential equation of the following form:

$$\frac{d\Theta_I}{dt} = -k_{I5}\Theta_I + k_{5I}\Theta_5, \quad (15)$$

taking into account that $\Theta_I + \Theta_5 = 1$. Final expressions for Θ_I and Θ_4 have the form of:

$$\begin{aligned} \Theta_I(t) &= \Theta_I(0)\exp(-t(k_{I5} + k_{5I})) + \\ &+ \frac{k_{5I}}{k_{I5} + k_{5I}}(1 - \exp(-t(k_{I5} + k_{5I}))); \\ \Theta_5(t) &= 1 - \Theta_I(t). \end{aligned} \quad (16)$$

Taking into account that between the rate constants k_{23} , k_{34} , k_{32} , k_{43} , and k_{15} , as well as between degrees of surface covering Θ_2 , Θ_3 , Θ_4 there is a relationship, we obtain expressions for the corresponding partial degrees of covering:

$$\begin{aligned} \Theta_2(t) &= \Theta_I(t)(1 + K_{23} + K_{23}K_{34})^{-1} = \Theta_I(t)\beta_2; \\ \Theta_3(t) &= \Theta_I(t)(1 + K_{32} + K_{34})^{-1} = \Theta_I(t)\beta_3; \\ \Theta_4(t) &= \Theta_I(t)(1 + K_{43} + K_{43}K_{32})^{-1} = \Theta_I(t)\beta_4. \end{aligned} \quad (17)$$

It should be noted that the coefficients β_i , appearing in (17), clearly do not depend on time. Nevertheless, such a dependence is still implicitly present, since in the potentiodynamic polarization regime β_i depends on E , and the potential varies linearly with time.

Let us differentiate expressions (17), i.e., find $\frac{d\Theta_i}{dt} = \frac{d(\Theta_i\beta_i)}{dt} = \beta_i \frac{d\Theta_i}{dt} + \Theta_i \frac{d\beta_i}{dt}$, where $i = 2, 3, 4$.

Since $\frac{d\beta_i}{dt} = \left(\frac{\partial\beta_i}{\partial E}\right)\left(\frac{\partial E}{\partial t}\right)$, for current densities, we

obtain expressions for the rates of partial anodic processes, and by summing them we would obtain a complete voltammogram (Fig. 6). Quite notably, that the use of this rather simplified, scheme allows us to obtain the i, E -dependence in which the rate of the anodic process between the second and third maxima no longer decreases to zero, as was previously (Fig. 3c), however, between the A3 and A4 maxima, the anodic current density in this case is zero, which contradicts the experiment. The position of the A2 maximum, as calculations show, does not depend on the potential scanning speed and alkali concentration, but the potentials of the A3 and A4 peaks with an increasing

c_{OH^-} shift to the more negative values (Fig. 6b), whereas with increasing v , the potentials noticeably improve.

Kinetic scenario (b)

Let us assume that an equilibrium distribution is established between states 1 and 2, as well as 3 and 4, while there is no equilibrium between states 2 and 3. Let us again combine the elementary states and the process diagram as follows:

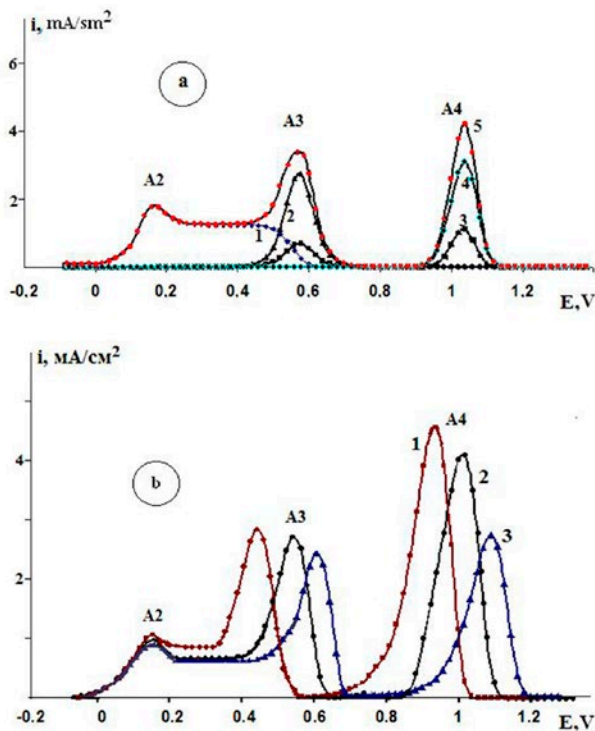
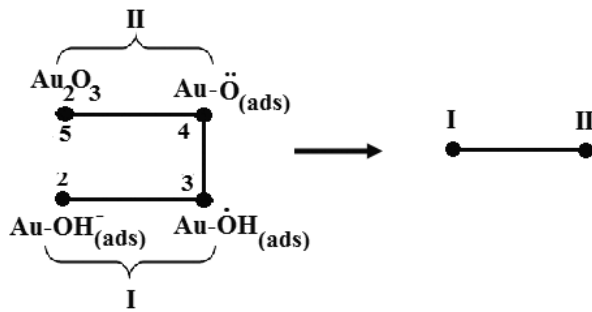


Fig. 6. (a) - Calculated velocities of partial anode processes i_1 (1), i_2 (2) i_3 (3) i_4 (4) and a voltammogram (5) obtained under the assumption that $c_{OH^-} = 0.1$ M and scanning rate of potential 0.6 V/sec; (b) – calculated voltammograms obtained in the Au|OH⁻, H₂O system at an alkali concentration 1.0 (1); 0.1 (2) 0.01 M (3) and $v = 0.6$ V/sec

Solving equations similar to (15) and carrying out the corresponding transformations, we again obtain the calculated i, E -dependencies (Fig. 7).

It appeared that such a process scheme already allows to obtain a non-zero current between the A3 and A4 maxima, but only when $v \geq 0.60$ V/s, although the current density values in this potential region are still much lower than those experimentally observed. The influence of v on the position of the A3 and A4 peaks is reflected correctly by the calculation. However, when $v \leq 0.4$ V/s, the A3 maximum practically disappears, and this, in principle, contradicts the experimental results [7].

4. Conclusions

The method of kinetic diagrams allows performing a fairly detailed analysis of stationary partial anodic processes in the Au|OH⁻, H₂O

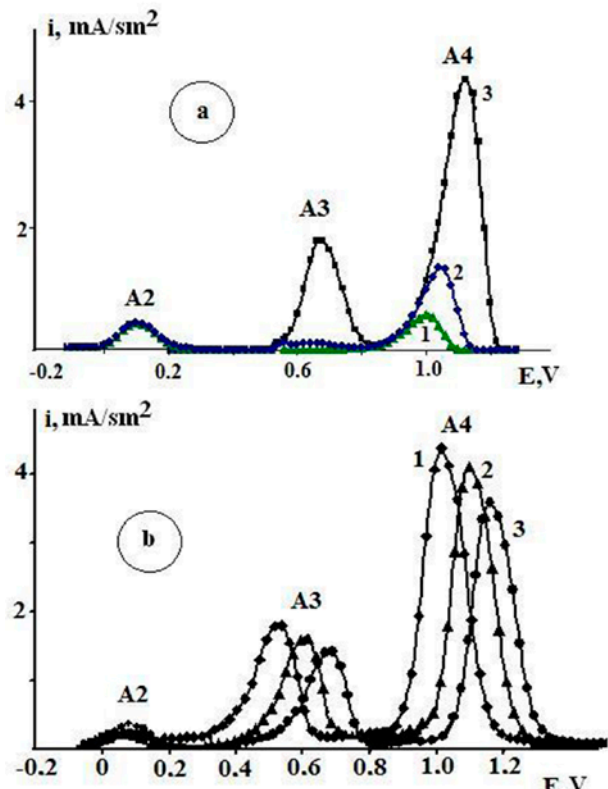


Fig. 7. a) Calculated voltammograms obtained according to the kinetic scenario scheme (b) at a potential scanning rate equal to 0.04 (1); 0.10 (2) and 0.60 (3) V/sec and an alkali concentration of 0.1 M; b) Calculated voltammograms obtained according to the kinetic scenario scheme (c) at a potential scanning speed equal to 0.60 V/sec and an alkali concentration of 1.0 (1); 0.1 (2) and 0.01 M (3)

system and also to identify the shape of the general stationary voltammogram by calculation methods. The latter is qualitatively consistent with the experimental one, which is also characterized by the presence of four main current peaks.

Within the framework of the basic assumption of the implementation of the Langmuir adsorption model, we calculated the stationary degrees of covering of the gold surface with various surface-active forms of oxygen as a function of the electrode potential. It was found that the change in the concentration of OH⁻ ions mainly affects the region of their adsorption potentials.

The formal equilibrium constants of individual electrode stages were calculated using the enumeration method. Their values correlate by the order of magnitude with the tabulated data [36], which indicates the correctness of our results.

Taking into account the non-stationary nature of processes occurring predominantly in the region of the A3 and A4 potentials' maxima on the voltammogram, in the general case requires consideration of seven different kinetic situations. For two of them, associated with the delayed formation of Au₂O_{3(ads)}, as well as with the heterogeneous transformation of the monoradical $\dot{O}H_{ads}$ to diradical \ddot{O}_{ads} , a qualitative agreement between the calculated and experimental data was found. It is mainly related to the nature of the influence of the scanning rate of the potential and the volume concentration of OH⁻ ions on the position and amplitude of the A3 and A4 peaks present on the anodic voltammogram of gold in an alkaline medium. However, it was not possible to establish complete correspondence between the shapes of the calculated and experimental voltammograms over the entire range of anodic potentials. This was probably due to the implementation of the mixed kinetics regime of the anodic oxidation of OH⁻ ions on Au, the consideration of which goes beyond the goals and objectives of this work.

Contribution of the authors

The authors contributed equally to this article.

Conflict of interests

The authors declare that they have no known competing financial interests or personal

relationships that could have influenced the work reported in this paper.

References

1. Zartcyn I. D., Shugurov A. E., Marshakov I. K. Thermodynamic coupling of anode and cathodic reactions in case of metal dissolution in the electrolytes. *Tambov University Reports. Series Natural and Technical Sciences*. 1997;2: 23–26. (In Russ., abstract in Eng.). Available at: <https://www.elibrary.ru/item.asp?id=16398081>
2. Zartcyn I. D., Shugurov A. E., Marshakov I. K. The anomalous dissolution of iron as a result of the chemical conjugation between iron ionization and hydrogen evolution. *Protection of Metals*. 2001;37(2): 138–143. <https://doi.org/10.1023/a:1010369904266>
3. Zartcyn I. D., Shugurov A. E., Marshakov I. K. Kinetics of chemically conjugate reactions of metal dissolution in the presence of oxidant. *Protection of Metals*. 2000;36(2): 140–145. <https://doi.org/10.1007/bf02758337>
4. Zhen C.-H., Sun S.-G., Fan C.-J., Chen S.-P., Mao B.-W., Fan Y.-J. In situ FTIRS and EQCM studies of glycine adsorption and oxidation on Au (111) electrode in alkaline solutions. *Electrochimica Acta*. 2004;49(8): 1249–1255. <https://doi.org/10.1016/j.electacta.2003.09.048>
5. Chun-Hua Z., Chun-Jie F., Yan-Juan G., Sheng-Pei C., Shi-Gang S. Adsorption and oxidation of glycine on Au film electrodes in alkaline solutions. *Acta Physico-Chimica Sinica*. 2003;19: 60–64. <https://doi.org/10.3866/pku.whxb20030114>
6. Beltowska-Brzezinka M., Łuczak T., Holze R. Electrocatalytic oxidation of mono- and polyhydric alcohols on gold and platinum. *Journal of Applied Electrochemistry*. 1997;27(9): 999–1011. <https://doi.org/10.1023/A:1018422206817>
7. Kraschenko T. G., Bobrinskaya E. V., Vvedenskii A. V., Kuleshova N. E. Kinetics of electrochemical oxidation of anion glycine on gold. *Condensed Matter and Interphases*. 2014;16 (1): 42–49. (In Russ., abstract in Eng.). Available at: <https://www.elibrary.ru/item.asp?id=21490889>
8. Goldshtein B. N., Volkenshtein M. V. Investigation of nonstationary complex monomolecular reactions by the graph method*. *Doklady of the USSR Academy of Sciences*. 1968;78: 386–388. (In Russ.)
9. Goldshtein B. N., Magarshak D. B., Volkenshtein M. V. Analysis of monosubstrate enzyme reactions by graph method*. *Doklady of the USSR Academy of Sciences*. 1970;191: 1172–1174. (In Russ.)
10. Goldshtein B. N., Shevelev E. A., Volkenshtein M. V. Stability analysis of enzyme systems with feedbacks by the graph method*. *Doklady of the USSR Academy of Sciences*. 1983;273: 486–488. (In Russ.)

11. Goldshtein B. N., Volkenshtein M. V. Simple kinetic models explaining critical phenomena in enzymatic reactions with enzyme and substrate isomerization*. *Doklady of the USSR Academy of Sciences*. 1988;22: 1381–1392. (In Russ.)
12. Štrbac S., Hamelin A., Adžić R. R. Electrochemical indication of surface reconstruction of (100), (311) and (111) gold faces in alkaline solutions. *Journal of Electroanalytical Chemistry*. 1993;362: 47–53. [https://doi.org/10.1016/0022-0728\(93\)80005-3](https://doi.org/10.1016/0022-0728(93)80005-3)
13. Chang S. C., Ho Y., Weaver M. J. Applications of real-time FTIR spectroscopy to the elucidation of complex electroorganic pathways: electrooxidation of ethylene glycol on gold, platinum, and nickel in alkaline solution. *Journal of the American Chemical Society*. 1991;113(25): 9506–9513. <https://doi.org/10.1021/ja00025a014>
14. Beltramo G. L., Shubina T. E., Koper M. T. M. Oxidation of formic acid and carbon monoxide on gold electrodes studied by surface-enhanced Raman spectroscopy and DFT. *ChemPhysChem*. 2005;6: 2597–2606. <https://doi.org/10.1002/cphc.200500198>
15. Martins M. E., Córdova O. R., Arvia A. J. The potentiodynamic electroformation and electroreduction of the O-containing layer on gold in alkaline solutions. *Electrochimica Acta*. 1981;26: 1547–1554. [https://doi.org/10.1016/0013-4686\(81\)85127-4](https://doi.org/10.1016/0013-4686(81)85127-4)
16. Bruckenstein S., Shay M. An in situ weighing study of the mechanism for the formation of the adsorbed oxygen monolayer at gold electrode *Journal of Electroanalytical Chemistry and Interfacial Electrochemistry*. 1985;188: 131–136. [https://doi.org/10.1016/s0022-0728\(85\)80057-7](https://doi.org/10.1016/s0022-0728(85)80057-7)
17. Burke L. D. Cunnane V. J., Lee B. H. Unusual postmonolayer oxide behavior of gold electrodes in base. *Journal of The Electrochemical Society*. 1992;139: 399–406. <https://doi.org/10.1149/1.2069230>
18. Vitus C. M., Davenport A. J. In situ scanning tunneling microscopy studies of the formation and reduction of a gold oxide monolayer on Au(111). *Journal of The Electrochemical Society*. 1994;141(5): 1291–1298. <https://doi.org/10.1149/1.2054912>
19. Goldshtein B. N., Zalkind Ts. I., Veselovskii V. I. Electrochemical adsorption of oxygen on a gold electrode in solutions of chloric and sulfuric acids*. *Soviet Electrochemistry*. 1973;9 (5): 699–702. (In Russ.)
20. Chen A., Lipkowski J. Electrochemical and spectroscopic studies of hydroxide adsorption at the Au(111) electrode. *The Journal of Physical Chemistry B*. 1999;103: 682–691. <https://doi.org/10.1021/jp9836372>
21. Vetter K. J. *Elektrochemische Kinetik*. Springer Berlin, Heidelberg; 1961. <https://doi.org/10.1007/978-3-642-86547-3>
22. Tremiliosi-Filho G., Gonzalez E. R., Motheo A. J., Belgsir E. M., Léger J.-M., Lamy C. *Journal of Electroanalytical Chemistry*. 1998;444: 31–39. [https://doi.org/10.1016/S0022-0728\(97\)00536-6](https://doi.org/10.1016/S0022-0728(97)00536-6)
23. Nechaev I. V., Vvedenskii A. V. Quantum chemical modeling of hydroxide ion adsorption on group IB metals from aqueous solutions. *Protection of Metals and Physical Chemistry of Surfaces*. 2009;45(4): 391–397. <https://doi.org/10.1134/s2070205109040029>
24. Patritio E. M., Olivera P. P., Sellers H. The nature of chemisorbed hydroxyl radicals. *Surface Science*. 1994;306: 447–458. [https://doi.org/10.1016/0039-6028\(94\)90085-x](https://doi.org/10.1016/0039-6028(94)90085-x)
25. Alonso C., Gonzalez-Velasco J. Study of the electrooxidation of 1,3-propanediol on a gold electrode in basic medium. *Journal of Applied Electrochemistry*. 1988;18: 538–545. <https://doi.org/10.1007/bf01022248>
26. Safronov A. U., Kristensen P. A. IR spectroscopic characteristics of the surface of the gold electrode in solutions with different pH*. *Soviet Electrochemistry*. 1990;26(7): 869–873. (In Russ.)
27. Kirk D. W., Foulkes F. R., Graydon W. F. The electrochemical formation of Au(I) hydroxide on gold in aqueous potassium hydroxide. *Journal of The Electrochemical Society*. 1980;127(10): 1069–1076. <https://doi.org/10.1149/1.2129819>
28. Icenhower D. E., Urbach H. B., Harrison J. H. Use of the potential-step method to measure surface oxides. *Journal of The Electrochemical Society*. 1970;117(12): 1500–1506. <https://doi.org/10.1149/1.2407359>
29. Štrbac S., Adžić R. R. The influence of OH- chemisorption on the catalytic properties of gold single crystal surfaces for oxygen reduction in alkaline solutions. *Journal of Electroanalytical Chemistry*. 1996;403: 169–181. [https://doi.org/10.1016/0022-0728\(95\)04389-6](https://doi.org/10.1016/0022-0728(95)04389-6)
30. Burke L. D. Scope for new applications for gold arising from the electrocatalytic behaviour of its metastable surface states. *Gold Bulletin*. 2004;37(1-2): 125–135. <https://doi.org/10.1007/bf03215520>
31. Dobberpuhl D. A., Johnson D. C. Pulsed electrochemical detection at ring of a ring-disk electrode applied to a study of amine adsorption at gold electrodes. *Analytical Chemistry*. 1995;67: 1254–1258. <https://doi.org/10.1021/ac00103a017>
32. Xiao Sun S.-G., Yao J.-L., Wu Q.-H., Tian Z.-Q. Surface-enhanced Raman spectroscopic studies of dissociative adsorption of amino acids on platinum and gold electrodes in alkaline solutions. *Langmuir*. 2002;18: 6274–6279. <https://doi.org/10.1021/la025817f>
33. Hill T. L. Studies in irreversible thermodynamic IV. Diagrammatic representation of steady state fluxes for unimolecular systems. *Journal of Theoretical Biology*. 1966;10: 442–459. [https://doi.org/10.1016/0022-5193\(66\)90137-8](https://doi.org/10.1016/0022-5193(66)90137-8)

34. Goldshtein B. N. *Kinetic graphs in enzymology*. Moscow: Nauka Publ.; 1989. 164 p. (In Russ.)

35. Volkenshtein M. V., Goldshtein B. N., Stefanov V. E. Investigation of nonstationary enzyme reactions. *Doklady of the USSR Academy of Sciences*. 1967;1: 52–58. (In Russ.)

36. Suhotin A. M. *Handbook of electrochemistry**. Moscow: Khimiya Publ.; 1981. 487 p. (In Russ.)

* *Translated by author of the article*

Информация об авторах

Ilya D. Zartsyn, Dr. Sci. (Chem.), Professor of the Department of Physical Chemistry of the Voronezh State University (Voronezh, Russian Federation).
zar-vrn@mail.ru

Alexander V. Vvedenskii, Dr. Sci. (Chem.), Full Professor of the Department of Physical Chemistry of the Voronezh State University (Voronezh, Russian Federation).

<https://orcid.org/0000-003-2210-5543>
alvved@chem.vsu.ru

Elena V. Bobrinskaya, Cand. Sci. (Chem.), Associate Professor of the Department of Physical Chemistry of the Voronezh State University (Voronezh, Russian Federation).

<https://orcid.org/0000-0001-7123-4224>
elena173.68@mail.ru

Oleg A. Kozaderov, Dr. Sci. (Chem.), Docent, Head of the Department of Physical Chemistry, Voronezh State University (Voronezh, Russian Federation).

<https://orcid.org/0000-0002-0249-9517>
ok@chem.vsu.ru

Received 28.03.2023; approved after reviewing 08.04.2023; accepted for publication 15.06.2023; published online 25.03.2023.

Translated by Valentina Mittova